JOURNAL OF MATERIALS SCIENCE 37 (2002) 3189–3198

# Enhancement in micro-fatigue resistance of UHMWPE and HDPE processed by SCORIM

A. Y. ZHANG, E. JISHENG, P. S. ALLAN, M. J. BEVIS
*Wolfson Centre for Materials Processes, Brunel University, Uxbridge, UB8 3PH, UK*

The tribological performance of UHMWPE and HDPE polymers, processed by a novel polymer process technology SCORIM (Shear-Controlled ORientation TEChnology) in injection moulding, shear controlled orientation in injection moulding (SCORIM) was evaluated against a through-hardened steel under different test conditions and compared with those processed by conventional injection moulding. Results indicate a significant improvement in the wear resistance using the SCORIM technology as a result of an increase in the mechanical properties. SEM microscopy shows a change of wear mechanisms dominated by micro-fatigue when using conventional injection moulding, compared to mild abrasive wear when using the SCORIM technology under the same test conditions. Examination of microstructure reveals the random aggregation of polymer molecules in the samples processed by a conventional injection moulding. Using the SCORIM technology, the molecules were sheared and orientated and a fibril microstructure formed as an *in situ* fibre reinforced composite. DSC analysis shows an increase in a second phase shish kebab structure in the samples processed by SCORIM technology. The fibril microstructure with an increase in shish kebab structure results in a significant improvement in wear resistance. Using the surface normal to the direction of the orientated molecular fibril microstructure as a contact surface, the possibility of the initiation and development of micro-cracks was reduced, especially the micro-cracks parallel to the contact surfaces. © *2002 Kluwer Academic Publishers*

## 1. Introduction

Polyethylene with long carbon-carbon chains, for instance ultra high molecular weight polyethylene (UHMWPE) or high density polyethylene (HDPE), has been widely applied for bearings because of its advantages of high wear resistance and low friction. Based on its excellent biological compatibility and high resistance to the biological environment, polyethylene has been used to manufacture acetabular cups against a stainless femoral component, which has been regarded as the gold standard for artificial human joints since 1960's [1, 2]. However, current research work indicates that micro-fatigue is one of the most important factors, which result in the failure of artificial human joints [3–6].

Fatigue wear is defined as the removal of particles detached by fatigue arising from cyclic stress variations. Wear due to surface fatigue is characterized by the initiation of cracks followed by crack propagation and pitting of materials under cyclic surface stresses. Work by Briscoe *et al.* [7] demonstrates that polyethylene has more pronounced viscoelastic properties when subjected to surface stresses during sliding of an indenter over a polyethylene surface. The deformation of polyethylene shows a peculiarly regular crack formation. This is due to the repeated effect of the squeezing of a material prow, which accumulates in front of the indenter until it reaches its elastic limit. A similar phenomenon is also reported using polymers on the micron scale by Khurshudov and Kato when observing under an atomic force microscope [8]. The stresses are concentrated near contact surfaces as described by Fisher and co-workers [9, 10]. Work by Wang and co-workers [6] illustrates that the micro-fatigue is attributed to the disconnection and breakage between UHMWPE molecules after orientation and softening of UHMWPE material on the contact surface.

It is well known that a high energy is required to break a C—C covalent bond. In other words, an improvement in the connection between UHMWPE molecules is one of the key factors to enhance fatigue wear resistance. In order to achieve it, two important technologies are currently applied: irradiation technology to cross-link UHMWPE materials [1] and fibre reinforcement technology [11]. Recent work by Choudhury and Hutchings [12] demonstrates an increase in micro-abrasive wear and the possibility of premature fracture of UHMWPE after irradiation. Work by Jacobs *et al.* [11] indicates that the a composite of HDPE reinforced by UHMWPE fibres creeps much less than UHMWPE and even less than HDPE. This allows for longer service periods of bearings.

Shear-Controlled ORientation TEChnology (SCORIM) is an advanced polymer processing technology [13–15]. In the application of SCORIM, polymer is sheared during solidification under controlled conditions, which results in *in situ* fibril reinforcement of engineering parts. Previous work [16–18] demonstrates an improvement in preferred orientation of polymer materials using SCORIM, which results in enhancement of stiffness and mechanical strength.

This paper concerns the use of SCORIM technology applied to injection moulding, shear controlled orientation in injection moulding (SCORIM) for the enhancement of micro fatigue wear resistance. The work is directed to an understanding of the microstructure effect on mechanical properties and tribological performance of polyethylene materials moulded by SCORIM and conventional injection moulding respectively.

## 2. Experimental procedure

### 2.1. Materials

Two polyethylene materials, provided by Hoechst AG, were used in this work. They were UHMWPE, Hostalen GUR 412 with an average molecular weight (Mw) of $3 \times 10^6$ and density of 0.936 g $cm^{-3}$, and HDPE, Hostalen GM 9522F with an average Mw of $0.22 \times 10^6$, density of 0.937 g $cm^{-3}$ and melt flow index of 0.6 g per 10 minutes. Five wt% UHMWPE was melt blended with HDPE using an intermeshing, co-rotating twin-screw extruder. The blending process is reported in Ref. 19.

Both SCORIM and conventional injection moulding technology were employed to produce test specimens from UHMWPE-HDPE blends with a diameter of 5 mm and 40 mm gauge length. The equipment and process technology are described in Ref. 19.

The steel, AISI 52100, was used to make a disc of 130 mm diameter for tribological experiments. It consists of 1.0 wt% carbon, 0.3 wt% Mn and 1.5 wt% Cr. The steel was through hardened and tempered to a hardness value of 750 kg $mm^{-2}$. The disc surface was ground with a roughness value of 0.3 $\mu$m (Ra).

### 2.2. Tribological tests

A conventional rotating pin-on-disc wear machine was employed to evaluate tribological performance. A configuration of the wear machine is described in Ref. 20. A polymer bar was cut at its central position into two specimens with a flat surface of 5 mm diameter as the contact surface in wear tests. A load was applied on a flat contact surface of pin specimens with a roughness of 0.25 $\mu$m (Ra), which is against a rotating steel disc specimen with a test track of 140 mm diameter at 150 rpm speed. The pin and disc specimens were cleaned respectively with solvents before testing. All tests were carried out under dry conditions in air at room temperature.

Two types of wear tests were carried out: a long term test and a step-load test. In a long term test, a constant load, 20 N or 40 N, was applied for a period of one hour. In a step-load test, a load varied at 2 N, 5 N then at a step of 5 N up to 75 N for each period of 15 minutes.

Friction force was continuously recorded in both types of tests on a chart paper using a calibrated linear variable differential transducer. Friction coefficient, $\mu$, was calculated by the friction force over the normal load applied. Wear was accessed by wear volume, $V$, and wear rate, $W_r$, was calculated from the wear volume over the sliding distance.

### 2.3. Evaluation of material properties

A tensile machine was used to evaluate mechanical properties of polymer specimens. A hardness tester was employed to measure a hardness value at 50 mN applied load (loading for 20 seconds and holding for 10 seconds). Using a standard method of ISO 1183, a density value of polymer specimens was determined.

### 2.4. Analysis

A Perkin Elmer DSC-7 was used to carry out thermoanalysis of polymer specimens using a heating rate of 10°C $min^{-1}$. Light microscope, SEM and TEM were employed to investigate the microstructure and wear mechanisms.

## 3. Results

### 3.1. Tribological behaviour during sliding

Wear performance was evaluated in long term sliding tests under two different applied loads. Fig. 1 shows that wear increased with an increase in sliding distance in two types of variation. There is an initial period of relatively high wear, referred to generally a running-in wear stage. A period of more gradual wear, an equilibrium wear stage, followed. In this work, the tribological performance at equilibrium stages was used to evaluate the influence of process technologies. Examination of Fig. 1 revealed that mild wear occurred under 20 N applied load for conventional and SCORIM specimens. Under 40 N applied load, the relatively mild wear existed using SCORIM and the severe wear using a conventional injection moulding technology. Fig. 2 gives wear rates at equilibrium stages from Fig. 1. Results indicated a reduction in the wear rates at one order of magnitude using SCORIM compared with conventional injection moulding technology. The wear resistance was significantly enhanced by the use of SCORIM.

Fig. 3 presents friction coefficients at an equilibrium wear stage in sliding tests. Results indicated that, using SCORIM, the friction coefficient was high compared with conventional injection moulding technology under 10 N applied load. However, it reduced at 40 N applied load.

### 3.2. Dependence on applied load

An investigation of the tribological performance was carried out under different applied loads. Figs 4 and 5 show the tribological behaviour of specimens moulded by both technologies respectively. Fig. 4 demonstrates that wear rates increased with an increase in applied loads. As in the above section, there was a significant enhancement in wear resistance of the materials using SCORIM compared with conventional injection moulding technology.

Examining Figs 4 and 5, it is evident that the tribological performance of both kinds of specimens behaved differently in a different range of applied loads. Under a low applied load, a low value of wear rate occurred without a distinguishable difference for each kind of specimen. However there was a dramatic reduction in the friction coefficient with an increase in applied loads,

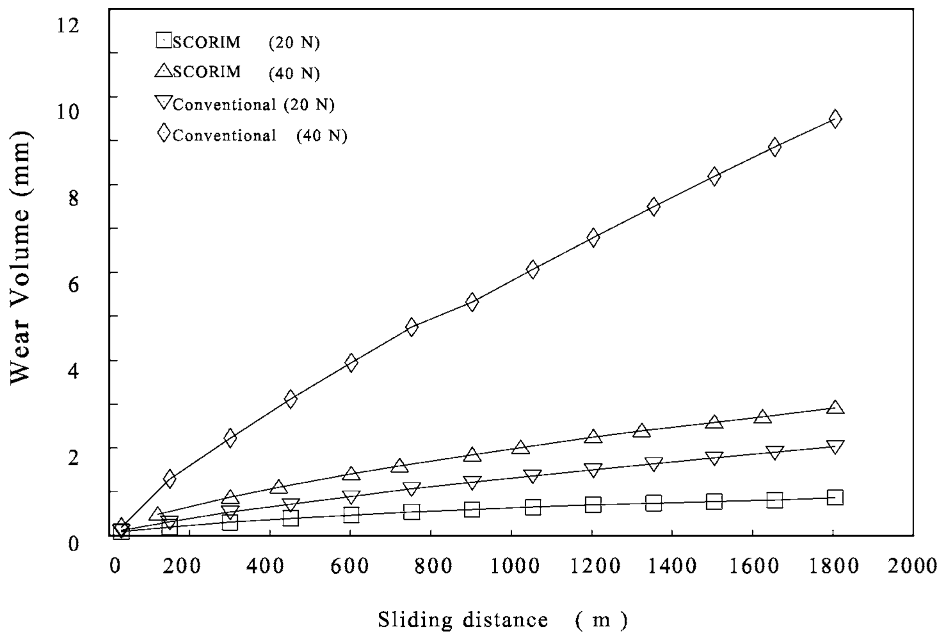


*Figure 1* Effect of different moulding technologies on wear behaviour during sliding tests.

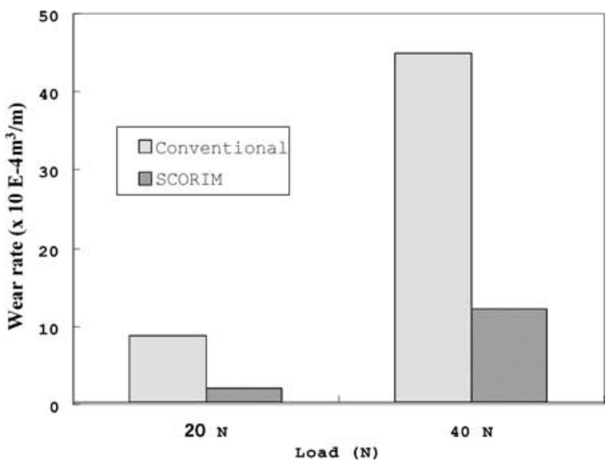


*Figure 2* Effect of moulding technologies on wear rates.

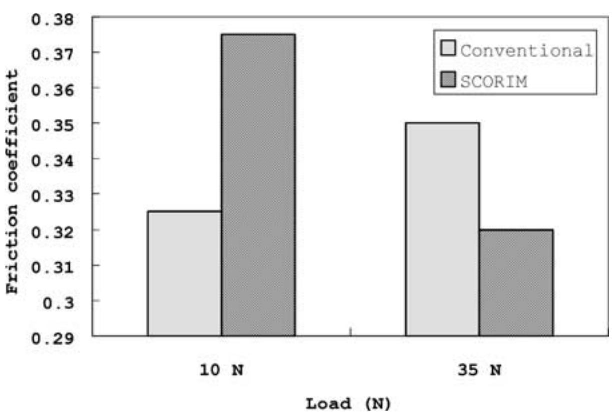


*Figure 3* Effect of moulding technologies on friction behaviour.

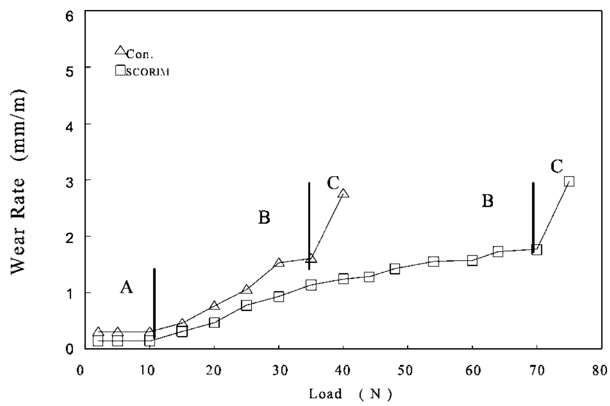


*Figure 4* Variation of wear behaviour with processing technology and applied load.

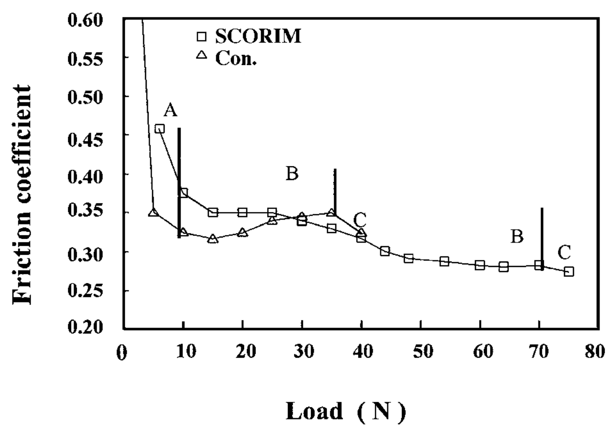


*Figure 5* Variation of friction behaviour with processing technology and applied load.

for range A shown in Figs 4 and 5. In range B, an increase in wear rate was observed for both the conventional and SCORIM specimens while a similar friction behaviour existed for the specimens moulded by a conventional injection moulding technology with an increase in applied load. A further moderate reduction appeared for those moulded by SCORIM, the range B.

Under a high applied load, wear increased substantially with little increase in applied loads while a reduction in friction coefficients took place, range C in Figs 4 and 5. In this work, the maximum applied load with a relatively low value of the wear rate was referred to as the load-carrying capacity. Fig. 6 indicated that the load-carrying capacity was over two times higher using

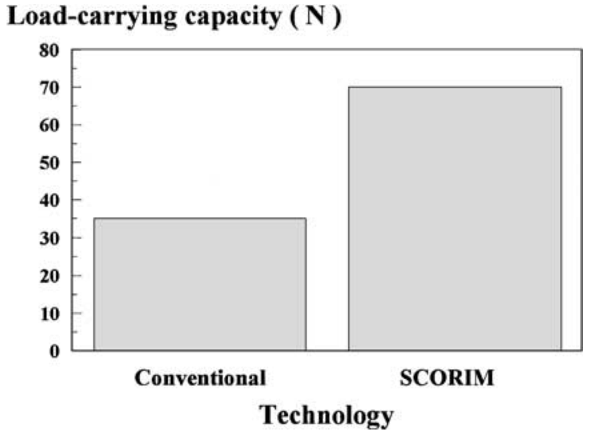


*Figure 6* Effect of moulding technologies on the load-carrying capacity.

SCORIM than using conventional injection moulding technology.

### 3.3. Wear mechanisms

Light microscopy was employed to examine wear mechanisms under different sliding conditions. Fig 7 shows the worn surfaces of specimens. Light micrographs in Fig. 7a and c illustrated that contact surfaces were abraded along a sliding direction. Consequently, a similar wear mechanism, mild abrasive wear, was one of the predominant wear mechanisms for the specimens moulded by both technologies respectively under 20 N applied load, and corresponded to a mild wear phenomenon in Figs 1, 2 and 4. However the abrasive wear phenomenon became relatively more severe on the worn surface for conventional injection moulded specimens, Fig. 7a, than specimens produced by SCORIM, Fig. 7c.

Under 40 N applied load, different phenomena existed using specimens moulded by different technologies. For a specimen moulded by conventional injection moulding technology, a large number of pits occurred on the worn surfaces, A in Fig. 7b. In the other words, the fatigue wear was one of the predominant wear mechanisms using conventional injection moulding technology. Using SCORIM, an abraded worn surface was observed under 40 N applied load on the test specimens, Fig. 7d, which indicated a predominant wear mechanism, mild abrasive wear and showed good agreement with low wear rates in the sliding tests, Fig. 2.

## 4. Discussion

Wear of polymer materials can be caused by many wear mechanisms, for example adhesion, abrasion, chemical reaction, fatigue and transferring attributed to adhesion. To investigate such a complex phenomenon, a simple classical theory is often used, known as Archard wear equation [21] as follows:

$$W_r = K\frac{L}{H} \tag{1}$$

where $W_r$ is the wear rate, $L$ the normal load on a surface, $H$ the hardness and $K$ is called dimensionless wear coefficient.

Fig. 8 shows the relationship between the wear rates and hardness of the specimens moulded by different technologies respectively. It is evident in Fig. 8 that the wear rate was inversely proportional to the hardness in sliding tests, which is in a good agreement with the Archard wear equation in Equation 1.

As described in the Section 3.3, one of the predominant wear mechanisms was micro-fatigue wear when using a conventional injection moulding technology in sliding tests. As an extreme case, an assumption can be made that a coefficient of fatigue wear may be interpreted as an inverse of the average number of loading cycles to break asperities or materials on the scale of polymer molecules. According to Manson-Coffin [22] low-cycle fatigue relation, $N_f$ , the number of loading cycles resulting in failure of the polymer material, can be given as follows:

$$N_f = \left(\frac{\sigma_f'}{\sigma_e'}\right)^m \tag{2}$$

where $\sigma_f'$ is the stress to failure in one loading cycle, $\sigma_e'$ the effective stress on the loaded surface and $m$ an index. Using the Equations 1 and 2, $K_f$, a coefficient of the fatigue wear, is obtained by:

$$K_f = C_f\left(\frac{\sigma_e}{\sigma}\right)^m \tag{3}$$

where $C_f$ is a constant depending on the tribological system, $\sigma_e$ the average effective stress on the loaded surface and $\sigma$ the stress at failure of materials. Fig. 9 gives a variation of wear rates with the stress at failure, $\sigma$, of the specimens moulded by the different technologies. Fig. 9 shows that the micro-fatigue wear resistance was enhanced significantly with an increase in the stress at failure using the SCORIM specimens in sliding tests. The coefficient of fatigue wear, $K_f$, is inversely proportional to the stress to failure of polymer material, which is in a good agreement with Equation 3.

Fatigue is a process, in which a crack is initiated and developed under the cyclic stresses. A reduction in the micro-voids and micro-cracks in specimens can result in an improvement in resistance to fatigue wear. Using SCORIM, the melt UHMWPE-HDPE blend material was sheared during solidification under controlled conditions. Additional UHMWPE-HDPE blend material can be added to the mould cavity to compensate for the shrinkage during solidification. Consequently, the specimens were produced with a reduction in internal defects such as micro-voids associated with the unsatisfactory packing of the mould. Evidence of a reduction in these internal defects is an increase in the density of the specimens produced using SCORIM compared with conventional injection moulding technology. Fig. 10 shows a variation in the wear rates and densities of specimens using the two different technologies. Using the same batch of raw material, the density of specimens increased from 0.95 g cm$^{-3}$ using the conventional injection moulding technology to 0.96 g cm$^{-3}$ using SCORIM.

In order to understand the enhancement in mechanical properties and tribological performance that result

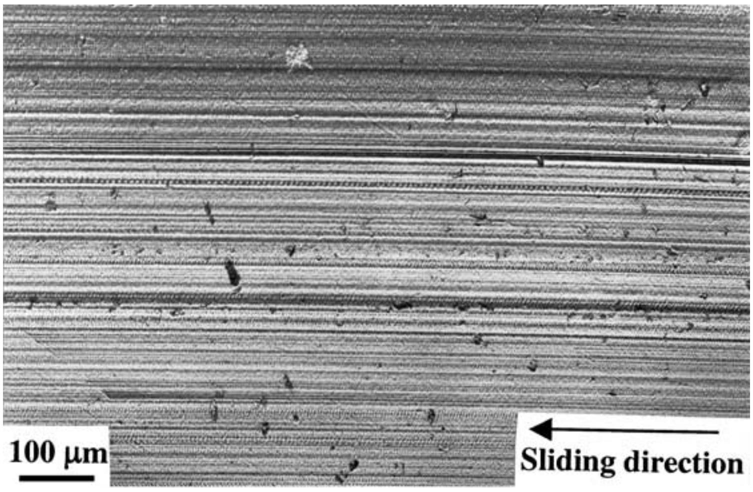


(a)

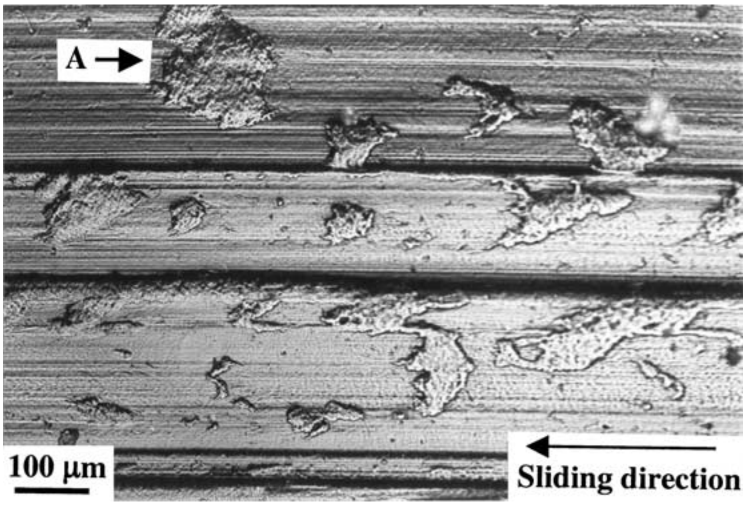


(b)

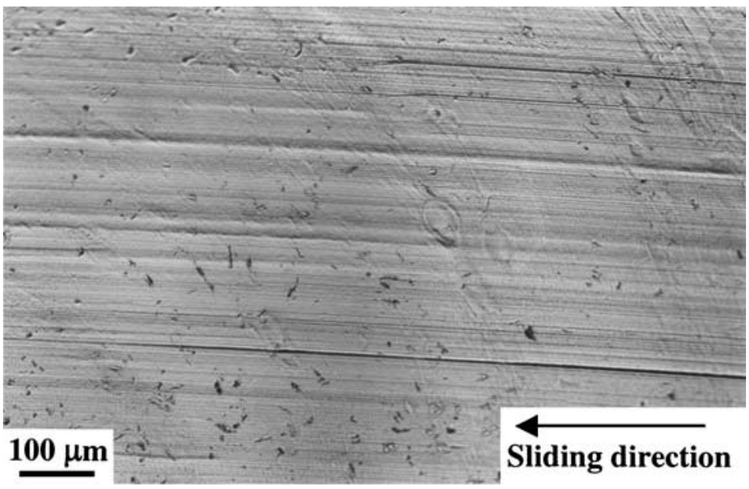


(c)

*Figure 7* Light micrographs of worn surfaces of the specimens moulded by conventional injection moulding technology (a and b) and by SCORIM (c and d) under 20 (a and c) and under 40 N applied loads (b and d). *(Continued.)*

from using SCORIM moulding technology, the macro- and the microstructure of the moulded specimens was investigated. The polished specimens were observed under a light microscope. It was found that two phases, a major and a minor phase, occurred in the specimens produced using conventional injection moulding technology, Fig. 11a and c. The minor phase represents the UHMWPE. The UHMWPE is a polymer with a high molecular weight of $1 \times 10^6$ and the HDPE with $1 \times 10^4$. They are carbon-hydrogen compounds with a large number of C—C covalent bonds as the backbone. Fig. 11a and c implies that the action of compounding and moulding has not entirely dispersed the particles of high molecular weight polyethylene. Examination of these specimens under SEM provides the further evidence of the retention in the specimens moulded by the

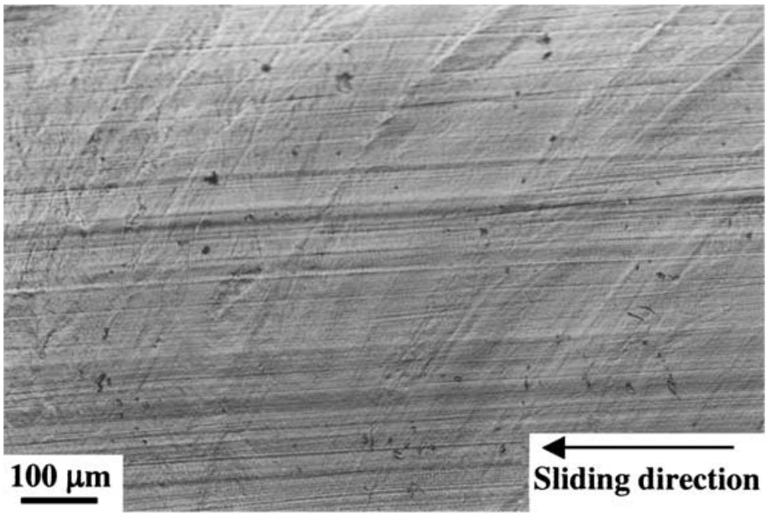


(d)

*Figure 7* *(Continued.)*

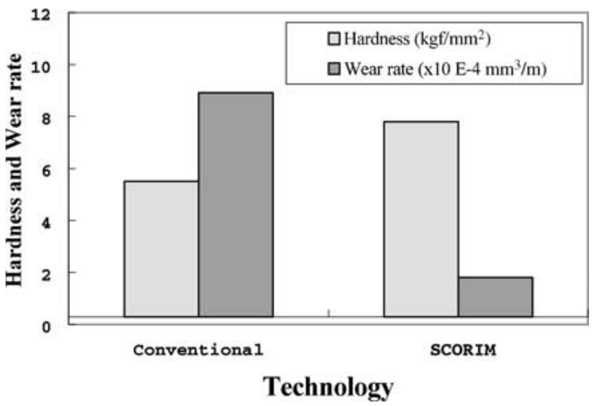


*Figure 8* Effect of SCORIM on the hardness and wear behaviour.

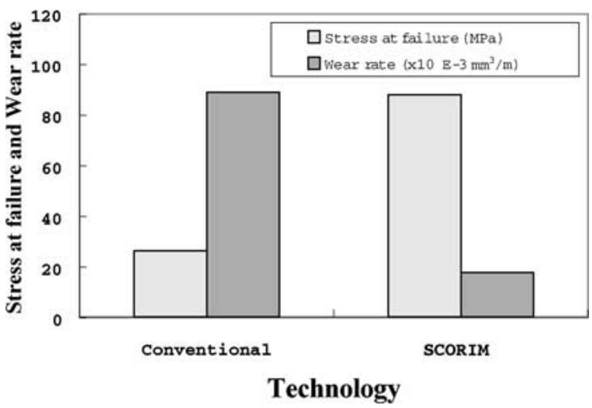


*Figure 9* Effect of the SCORIM on the stresses at failure and the wear behaviour.

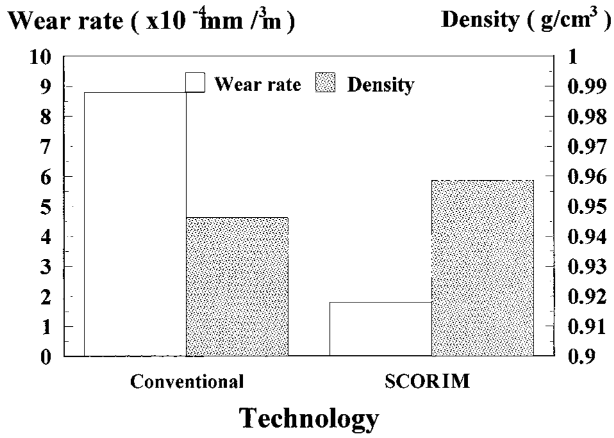


*Figure 10* Effect of the SCORIM on the density and wear behaviour.

conventional injection moulding technology, not only in the macro- but also in the microstructure, Fig. 12a.

The retention of large UHMWPE particles could result in two phenomena. Firstly, the particles give low ratio of molecule surface area to volume. The mechanical properties and wear resistance of engineering polymer materials are greatly affected by the connections between the large polymer molecules. In general, it is believed that three important types of connections exist in the engineering polymer materials. They are chemical cross-links, mechanical entanglements and molecular ties between the large polymer molecules. As an inert organic substance, polyethylene molecules are mainly connected to one another by mechanical entanglements and molecule ties in a general process. A low value of the molecular surface area of the retained UHMWPE and HDPE results in the low number of the connections between the molecules, and results in a decrease in the mechanical properties and wear resistance.

Secondly, micro-voids and micro-cracks formed during the moulding of specimens. They could easily exist at an interface between the retained UHMWPE and HDPE. During a tribological test, the micro-cracks were initiated from the micro-voids and developed under stresses at the interface, which result in fatigue wear, Fig. 7b.

Observation of the structure of SCORIM mouldings revealed that the UHMWPE appeared in the form of long fibres (Fig. 11b and d), rather than spherical retained particles (Fig. 11a and c). SEM illustrates the formation of a microstructure of *in situ* micro-fibres during the moulding process using SCORIM, Fig. 12b.

The microstructure of polymer composites reinforced by the *in situ* micro-fibres provides three advantages. Firstly, the fibril microstructure resulted in a significant increase in the possibility of connecting molecules with one another, which in turn improved

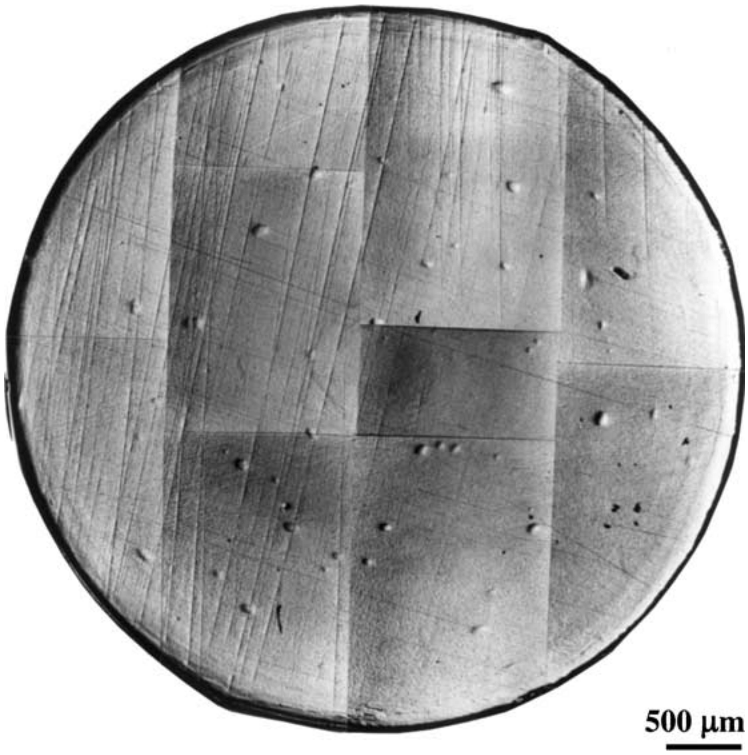


(a)

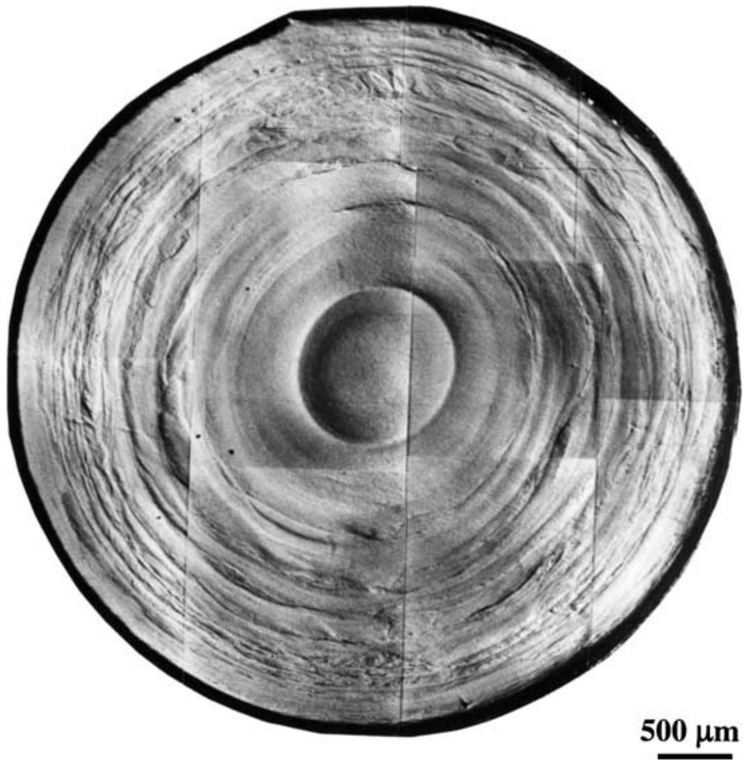


(b)

*Figure 11* Light micrographs of the cross sections (a and b: parallel to; c and d: transverse to a contact surface) of specimens moulded by conventional injection moulding (a and c) and by SCORIM (b and d). *(Continued.)*

mechanical properties and tribological performance of UHMWPE-HDPE blend materials, Figs 8 and 9.

Secondly, the micro-fibrils and the matrix were of the same kind of materials—polyethylene, which resulted in a significant enhancement in fibre-matrix adhesion, attributed to epitaxial crystallization and the molecular continuity of the phases.

Finally, a significant transformation of the crystalline microstructure took place. DSC investigation revealed the appearance of a second peak, which is related to the extended-chain of shish kebabs [17, 18] in the specimens moulded by SCORIM, Fig. 13. TEM microscopy illustrates that the crystalline morphology consists predominantly of randomly orientated lamella in the specimens moulded by conventional injection moulding, Fig. 14a. A clear orientated microstructure appeared using SCORIM, Fig. 14b. This microstructure is reported as a shish kebab microstructure [17, 18]. A shish

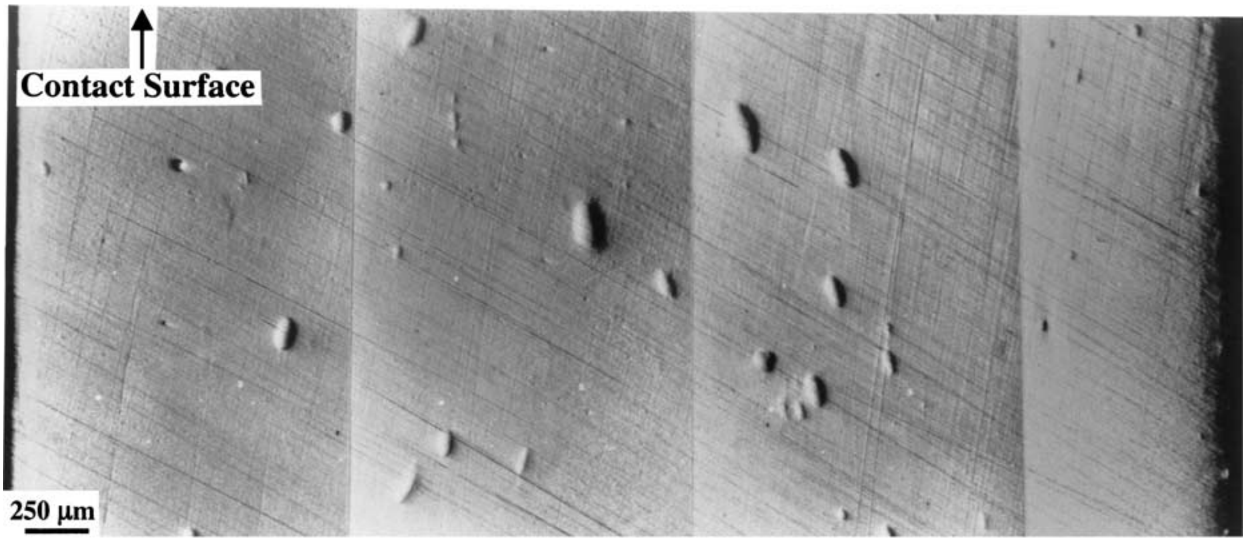


(c)

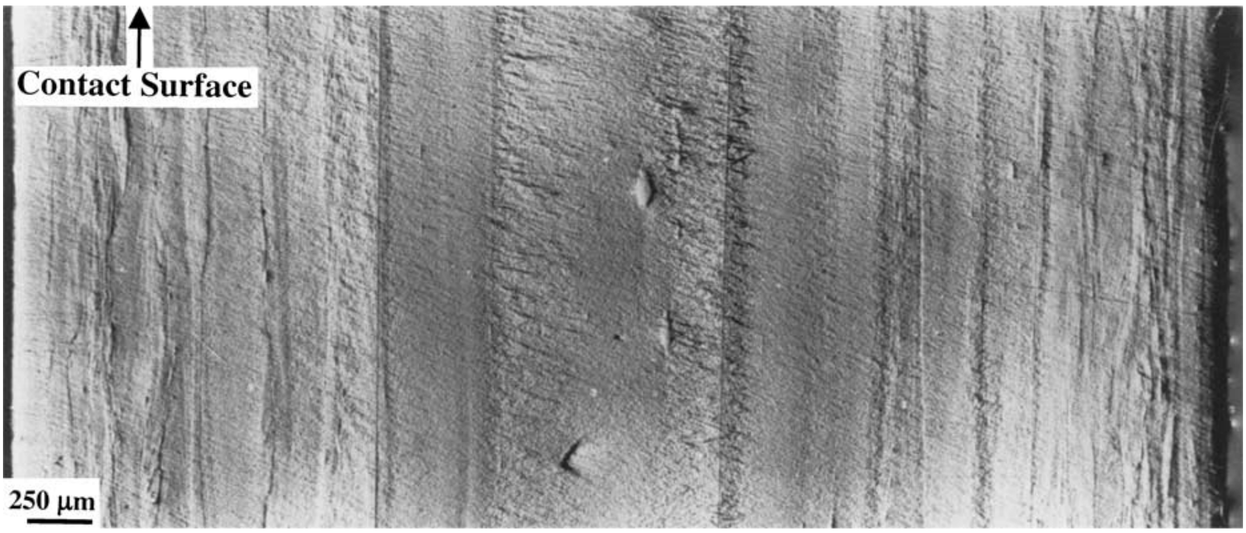


(d)

*Figure 11 (Continued.)*

kebab microstructure is described as a microstructure in which the extended-chains are on a backbone, the shishes A-A in Fig. 14c. In Fig. 14b, it is illustrated that the shishes of shish kebabs were parallel one another in a direction A and the folded-chains kebabs in a direction B. The enhancement of physical properties is accounted for by the formation of shishes and by the existence of interlocking kebabs, Fig. 14d.

For an application to tribology, one can use the surface transverse to a direction of *in situ* microfibres as the contact surface against the counterface in tribological applications. In this case, three phenomena could occur on a contact surface in tribological tests. First of all, the large molecules like long fibres acted as the main frame structure to support the higher load applied on specimens as a result of an increase in the load-carrying capacity, Figs 5 and 6. When one surface slides against another surface, the friction heat is generated on the contact surfaces. Polymer materials exhibit low heat conductivity. Polymer materials near the contact surfaces can melt by the friction heat during sliding tests under dry conditions. For the polymer composite reinforced by the *in situ* microfibres, one end of the long polymer molecules near the contact surface melted due to the friction heat in the tribological tests. However, another end of the molecules underneath the contact surfaces was still in the form of microfibre structures. This implies that they were well connected to one another and exhibited low wear rates and high load-carrying capacity in the tribological tests, Figs 1, 2 and 4. At the same time, the *in situ* microfibres could contact with the counterface as a result of abrasive wear on steel discs in tribological tests, Fig. 15. In fact, the *in situ* microfibres can clean the surface of counterface material, which results in an improvement in the formation of a transferring polymer film. The work reported by Briscoe [23] and Lancaster [24] illustrates that the thinner and better the transferring film forms on the counterface material, the lower the wear rates and the friction coefficients as shown in Figs 1 to 5.

For the second phenomenon, using SCORIM, the small molecules near the contact surfaces are melted attributed to the friction heat under the applied load. It is reported that the melted polymer materials can lubricate the contact surfaces that results in a low friction coefficient in tribological tests, as shown at stage A under low applied loads in Fig 5. At stage B, the situation was the same as at stage A for the specimens moulded

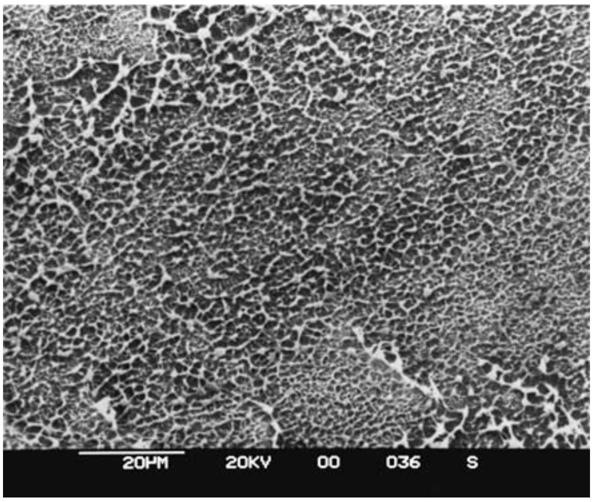


(a)

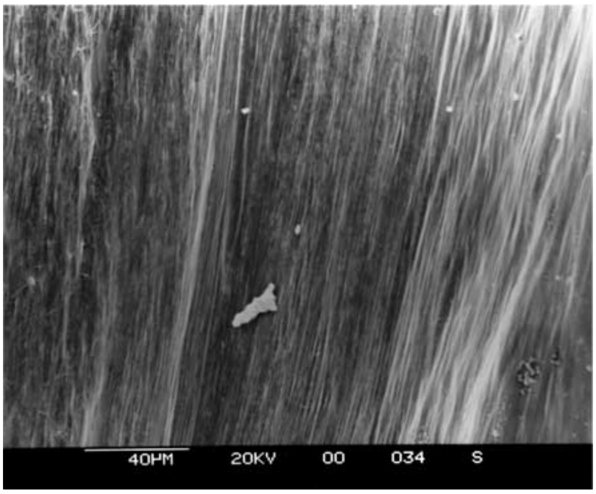


(b)

*Figure 12* SEM micrographs of the cross sections of the specimens moulded by (a) conventional injection moulding and (b) SCORIM.

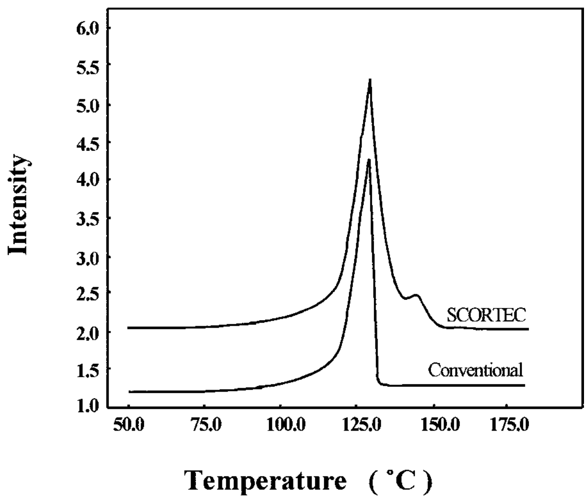


*Figure 13* DSC spectra of the specimens moulded by different moulding technologies.

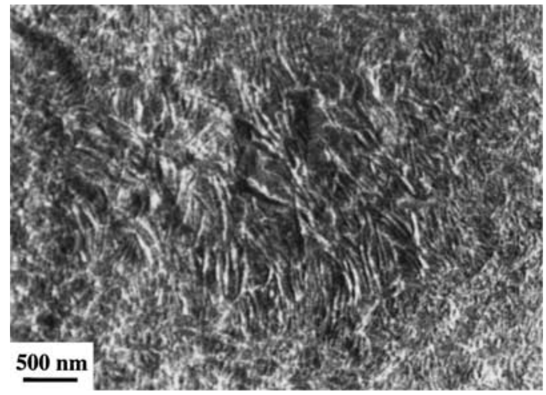


(a)

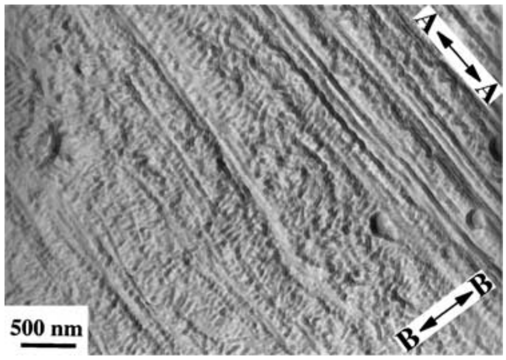


(b)

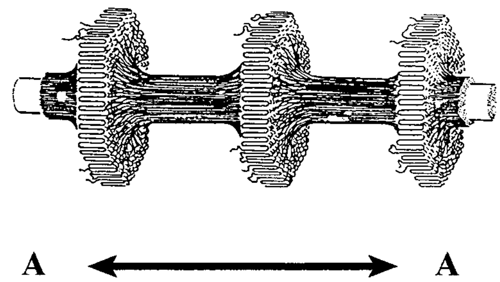


(c)

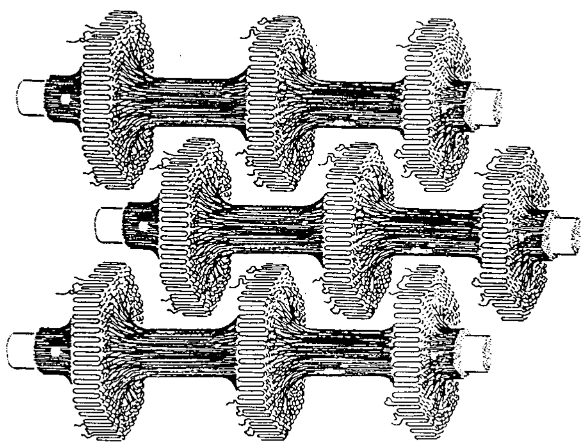

(d)

*Figure 14* TEM micrographs of (a) the random lamellar, formed in conventional injection moulding, and (b) the shish kebab microstructure, formed in SCORIM, of polyethylene and (c and d) the schematic illustration of shish kebabs.

by SCORIM, and showed similar friction behaviour in both stages. However, the retained polyethylene was worn away at a high rate from the conventional samples. This is attributed to the weak connections between the polyethylene phase in the specimens moulded by the conventional injection mouldings. This result is supported by the high wear rates and low friction values shown in, Figs 1, 4 and 5.

Finally, micro-cracks generally form and develop beneath the contact surfaces under stresses in tribological tests. Using the surface normal to the direction of the orientated molecular fibril microstructure as a

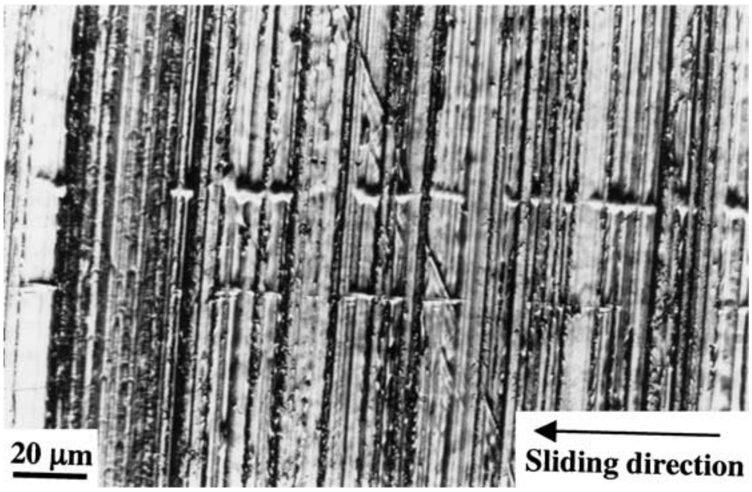


*Figure 15* Light micrographs of worn surfaces of the steel counterfaces against polyethylene specimens moulded by SCORIM.

contact surface, the possibility of the initiation and development of micro-cracks was reduced, especially the micro-cracks parallel to the contact surfaces. This implies a significant enhancement in the fatigue wear resistance in sliding tests using the specimens produced by SCORIM mouldings.

## 5. Conclusions

1. Using shear controlled orientation moulding technology (SCORIM), the predominant wear mechanism is transformed from a fatigue wear mechanism in the test specimens moulded by a conventional injection moulding to a moderate abrasive wear in sliding tests under a high applied load. This is attributed to a reduction in the formation of micro-voids and micro-cracks during the processing of specimens using SCORIM.

2. A significant enhancement in the wear resistance is achieved using SCORIM compared with using conventional injection moulding technology.

3. Wear resistance increases with an increase in the hardness and stress at failure of the specimens moulded by the different process technologies.

4. The microstructure of the *in situ* microfibre reinforced composite forms in the UHMWPE-HDPE blends during processing by SCORIM and results in a significant enhancement in wear resistance, load-carrying capacity and mechanical properties.

## Acknowledgement

The authors greatly appreciate the technical support from colleagues in the Wolfson Centre for Materials Processing, Brunel University.

## References

1. D. DOWSON, The James Clayton Memorial Lecture 2000, An ordinary meeting of the Institution held at IMechE Headquarters, London, on Wednesday 28 June 2000.
2. *Idem.*, in New Directions in Tribology, the First World Tribology Congress, IMechE (MEP Ltd, London, 1997) p. 3.
3. S. H. TEOH, *International Journal of Fatigue* **22** (2000) 825.
4. D. DOWSON, in "ASM Handbook, Vol. 18: Friction, Lubrication and Wear Technology," edited by Peter J. Blau (ASM International, 1992) p. 656.
5. H. A. MCKELLOP, P. CAMPBELL, SANG-HYUN PARK, T. P. SCHMALZRIED, P. GRIGORIS, H. C. AMSTUTZ and A. SARMIENTO, *Clinical Orthopaedics and Related Res.* **311** (1995) 3.
6. A. WANG, A. ESSNER, V. K. POLINENI, D. C. SUN, C. STARK and J. H. DUMBLETON, in New Directions in Tribology, the First World Tribology Congress, IMechE (MEP Ltd, London, 1997) p. 443.
7. B. J. BRISCOE, P. D. EVANS, E. PELILLO and S. K. SINBA, *Wear* **200** (1996) 137.
8. A. KHURSHUDOV and K. KATO, *ibid.* **205** (1997) 1.
9. J. R. COOPER, D. DOWSON and J. FISHER, *ibid.* **162–164** (1993) 378.
10. P. S. M. BARBOUR, D. C. BARTON and J. FISHER, *ibid.* **181–183** (1995) 250.
11. O. JACOBS, N. MENTZ, A. POEPPEL and K. SCHULTE, *ibid.* **224** (2000) 20.
12. M. CHOUDHURY and I. M. HUTCHINGS, *ibid.* **203–204** (1997) 335.
13. P. S. ALLAN and M. J. BEVIS, British Patent 2170-140-B, 1987.
14. *Idem.*, *Plastics and Rubber Processing and Applications* **7** (1987) 3.
15. P. S. ALLAN, M. J. BEVIS, J. R. GIBSON, C. J. MAY and I. E. PINWILL, *J. Materials Processing Technology* **56** (1996) 272.
16. P. S. ALLAN, S. A. HASHEMI, A. FAULKNER and M. J. BEVIS, *Plastics, Rubber and Composites Processing and Application* **27**(9) (1998) 407.
17. P. J. BARHAM and A. KELLER, *J. Mater. Sci.* **19** (1984) 3713.
18. Z. BASHIR, A. A. ODELL and A. KELLER, *ibid.* **21** (1986) 3993.
19. A. ZHANG, Ph.D. thesis, Brunel University, London, 1998.
20. E. JISHENG and D. T. GAWNE, *Wear* **213** (1997) 123.
21. J. F. ARCHARD, *J. Appl. Phys.* **24** (1953) 981.
22. J. F. TAVERNELLI and L. F. COFFIN, *Trans. ASM* **51** (1959) 438.
23. B. J. BRISCOE, *Tribology International* **14** (1981) 231.
24. J. K. LANCASTER, in "Polymer Science: A Materials Science Handbook," edited by A. D. Jenkins (North Holland, 1972) p. 959.

*Received 23 August 2001*
*and accepted 28 February 2002*